



Investigation of adsorption isotherms and rotational speeds for low temperature regeneration of desiccant wheel systems

Rang Tu^a, Yunho Hwang^{b,*}, Tao Cao^b, Mingdong Hou^a, Hansong Xiao^a

^aSchool of Civil and Resource Engineering, University of Science and Technology Beijing, Beijing 100083, China

^bCenter for Environmental Energy Engineering, University of Maryland, College Park, MD 20742, USA



ARTICLE INFO

Article history:

Received 17 August 2017

Revised 19 October 2017

Accepted 5 November 2017

Available online 21 November 2017

Keywords:

Desiccant wheel

Isotherm, Shape factor

Adsorption capacity

Rotational speed

Regeneration temperature

ABSTRACT

Effects of adsorption isotherms, namely shape factor and maximum adsorption capacity, and rotational speed on regeneration temperature of desiccant wheel systems are investigated. Higher maximum adsorption capacity is beneficial for reducing regeneration temperature especially for deep dehumidification of single-stage systems under humid climate, while the influence is not obvious with small dehumidification capacity. Higher shape factor (-1) is recommended for dehumidification at high relative humidity, while lower shape factor is better for low relative humidity. Rotational speed in the range of $10\text{--}15 \text{ r h}^{-1}$ is advised for single and two-stage systems under a wide range of working conditions for both deep and regular dehumidification applications when wheel thickness is 0.2 m and maximum adsorption capacity is 0.8 kg kg^{-1} . The reasons for different requirements of shape factor for regular and deep applications are discussed theoretically. Rotational speed ranges for different wheel thickness and maximum adsorption capacity are recommended.

© 2017 Elsevier Ltd and IIR. All rights reserved.

Étude des isothermes d'adsorption et des vitesses de rotation pour la régénération à basse température des systèmes de roues déshydratantes

Mots-clés: Roue déshydratante; Isotherme; Facteur de forme; Capacité d'adsorption; Vitesse de rotation; Température de régénération

1. Introduction

Solid desiccant wheel is an effective air processing component instead of low-dew point dehumidification. Thermal energy in a certain temperature range is used to regenerate the desiccant wheel for continuous air dehumidification. Therefore, the required regeneration temperature (t_{reg} , temperature of regeneration air entering desiccant wheels) is a key factor affecting selection of heat sources and performances of desiccant wheel systems. With the same dehumidification requirements, lowering t_{reg} is essential for the utilization of low grade waste heat or renewable energy.

t_{reg} is determined by a variety of factors, such as desiccant wheels' dimensions (Cao et al., 2014), structure of air channels (Zhang, 2008), rotational speed (Cao et al., 2014; Tu et al., 2013b;

Ruivo et al., 2015), inlet states of process and regeneration air (Tu et al., 2014; Ruivo et al., 2014), mass flow rate of regeneration air (Tu et al., 2015a), area ratio of regeneration section (Tu et al., 2014; Chung et al., 2009), purge section (Yadav and Yadav, 2016) and adsorption materials' properties (Al-Alili et al., 2015). It was reported that under the same wheel dimensions and working conditions, the lowest t_{reg} can be achieved by using equally divided desiccant wheels when two air streams have the same mass flow rate (Tu et al., 2015a). Besides, t_{reg} is also significantly influenced by system designs. It is suggested to adopt pre-cooling (Tu et al., 2015a) and cooling devices are preferred to be indirect evaporative cooling or heat exchangers other than direct evaporative cooling (Tu et al., 2015b, 2016; Jain and Dhar, 1995). It is found that t_{reg} can be reduced from over 110°C of systems with direct evaporative cooling to around 70°C of systems with indirect cooling under the discussed working conditions (process air inlet: 33°C and 19 g kg^{-1} , supply air: 10 g kg^{-1}) (Tu et al., 2016). Multi-stage desiccant de-

* Corresponding author.

E-mail address: yhwang@umd.edu (Y. Hwang).

Nomenclature

A	area
a	pore radius, m
BSC	Beijing Summer Condition
WSC	Washington airport Summer Condition
C	shape factor of desiccant material
COP	Coefficient of Performance
c_p	specific heat, $\text{kJ kg}^{-1} \text{K}^{-1}$
d_h	hydraulic diameter, m
D_A	ordinary diffusion coefficient, $\text{m}^2 \text{s}^{-1}$
D_S	surface diffusion coefficient, $\text{m}^2 \text{s}^{-1}$
f	area ratio, dimensionless
G	volume flow rate, $\text{m}^3 \text{s}^{-1}$
h	heat transfer coefficient, $\text{kW m}^{-2} \text{K}^{-1}$
h_m	mass transfer coefficient, $\text{kg m}^{-2} \text{s}^{-1}$
h_v	heat of vaporization, kJ kg^{-1}
k	thermal conductivity, $\text{kW m}^{-1} \text{K}^{-1}$
L	wheel thickness, m
Le	Lewis number
m	mass flow rate, kg s^{-1}
M	mass of desiccant wheel, kg
Nu	Nusselt number
ORS	Optimal Rotational Speed
Pa	standard atmospheric pressure, Pa
P_{vs}	saturated vapor pressure, Pa
P	process air
R	regeneration air
r_s	adsorption or desorption heat, kJ kg^{-1}
RS	Rotational Speed
t	Celsius temperature, oC
u	velocity, m s^{-1}
W	adsorption capacity of desiccant materials, $\text{kg}_{\text{water}} \text{kg}_{\text{dry adsorbent}}^{-1}$
x	volume ratio of adsorption material
x^*	mass ratio of adsorption material
Z	thickness, m
<i>Greek symbols</i>	
ω	humidity ratio, g kg^{-1}
φ	relative humidity ratio
τ	time
ρ	density, kg m^{-3}
σ	porosity
ξ	tortuosity factor, dimensionless
<i>Subscripts</i>	
a	air
ave	average
ad	adsorption material
c	cold
d	desiccant material
p	process
reg	regeneration
in	inlet
out	outlet
max	maximum
min	minimum
w	water
DW	desiccant wheel

in each stage. In this way, the desiccant material works at relatively high water content and be regenerated at a lower temperature. As the increase of stage number, air handling processes will be closer to those of inner cooling desiccant beds (Tu et al., 2013b, 2015a). Tu et al. (2015a, 2015d) has conducted thorough investigations to explain influences of stage number on t_{reg} and suggested optimal stage number when different cooling and heating fluids are adopted. Other researches (Zhang and Niu, 1999; Chen et al., 2016a) showed that t_{reg} could be reduced to about 60 °C.

This makes the adoption of low grade heat possible. Tu et al. (2014) investigated a heat pump driven two-stage desiccant wheel system, showing that t_{reg} can be reduced to lower than 50 °C with 10 g kg⁻¹ supply humidity ratio and coefficient of performance (COP) can be 4.3 and 7.3 under Beijing summer condition and AHRI (The Air-Conditioning, Heating, and Refrigeration Institute) summer condition.

Apart from system configuration study, developing novel desiccant materials has attracted many attention. It is suggested that desiccant wheels with lower specific heat and lower thermal conductivity are beneficial for dehumidification (Tu et al., 2013a). Novel adsorption materials, such as silica gel-polymer composite desiccant (Chen et al., 2016a), silica gel-lithium chloride composite desiccant (Jia et al., 2006b), and polymer-alumina composite desiccant (Chen et al., 2016b) have been developed. Jia et al. (2006a) reported that the composite material, which is the mixture of silica and lithium chloride, can remove 50% more moisture than silica gel. Polymer has been widely studied as an effective alternatives of silica gel for superabsorbent property. It is found by White et al. (2011) that zeolite and a superabsorbent polymer were more effective in dehumidification than silica gel at low regeneration temperature (50 °C) and high relative humidity (>60%). And test results of Lee and Lee (2012) showed that a superabsorbent polymer had two to three times higher sorption capacity than that of silica gel. Ge et al. (2010) studied the application of silica gel-haloid composite desiccant adopted in two-stage desiccant wheel cooling systems. Cao et al. (2014) investigated the performance of thin polymer DWs (30, 50 and 70 mm) at low regeneration temperatures (40, 50 and 60 °C), and reported that a 50 °C regeneration temperature was the optimum working condition because it can provide good moisture removal capacity (MRC) and latent COP simultaneously.

Compared with single stage systems, air in two-stage systems is handled in a higher relative humidity range. Besides, for deep dehumidification application, air is treated in a lower relative humidity range as compared with the regular dehumidification application. Therefore, recommended physical parameters for desiccant materials applied for low relative humidity dehumidification and high relative humidity dehumidification should be analyzed. Effects of the adsorption isotherms on the regeneration temperature of single stage and two-stage desiccant wheel systems under humid- and mild-climate for regular and deep dehumidification applications are discussed in this paper through simulation. Moreover, effects of rotational speed are taken into consideration. The results provide guidelines for selecting desiccant materials regarding shape factor, maximum water capacity, and rotational speed ranges for low temperature regeneration of desiccant wheel dehumidification systems.

2. Mathematical model and experiment validation of the desiccant wheel

2.1. Mathematical model

Transient heat and mass transfer processes happen between the air and the desiccant material across the air channels of desiccant wheels. These processes can be numerically described by four gov-

humidification systems have been a hot topic for the reduction of t_{reg} as compared with the single stage desiccant wheel system (Tu et al., 2014, 2015a, 2015c, 2017; Ge et al., 2010). Process air is dehumidified by the desiccant wheel and cooled by the cooling coil

Table 1

Literature review of commonly used adsorption isotherm equations for silica-gel.

(1)	$\phi = 0.0078 - 0.05759W + 24.16554W^2 - 124.478W^3 + 204.226W^4$ (Pesaran, 1980)
(2)	$\phi = -0.02833 + 8.18612W - 41.7964W^2 + 82.9974W^3$ (Ramzy and Kadoli, 2011)
(3)	$W = 0.24\phi^{2/3}$ (Kodama et al., 2001)
(4)	$W = 0.77\phi - 0.38\phi^2$ (Pesaran, 1983)
(5)	$\phi = (2.112W)^{r_s/h_v} (29.91P_{fg})^{r_s/h_v-1}$ (Vandenbulck et al., 1985)
(6)	$\phi = \frac{(0.616238W + 16.7916W^2 - 74.34228W^3 + 116.6834W^4)}{(1-(t-40)/300)}$ (Jeong et al., 2010)
(7)	$\phi = S_1 t W^2 + S_2 t W + S_3 W^4 + S_4 W^3 + S_5 W^2 + S_6 W$ (Dupont et al., 1994)
(8)	$W = 0.0329 - 0.4113 \times 10^{-5} t^2 + 0.0105 \times 10^{-3} \phi^2 + 0.6586 \times 10^{-6} \phi^3 + 0.7894 \times 10^{-10} t^3 \phi^2 + 0.6747 \times 10^{-12} t^3 \phi^3$ (Majumdar and Worek, 1989)

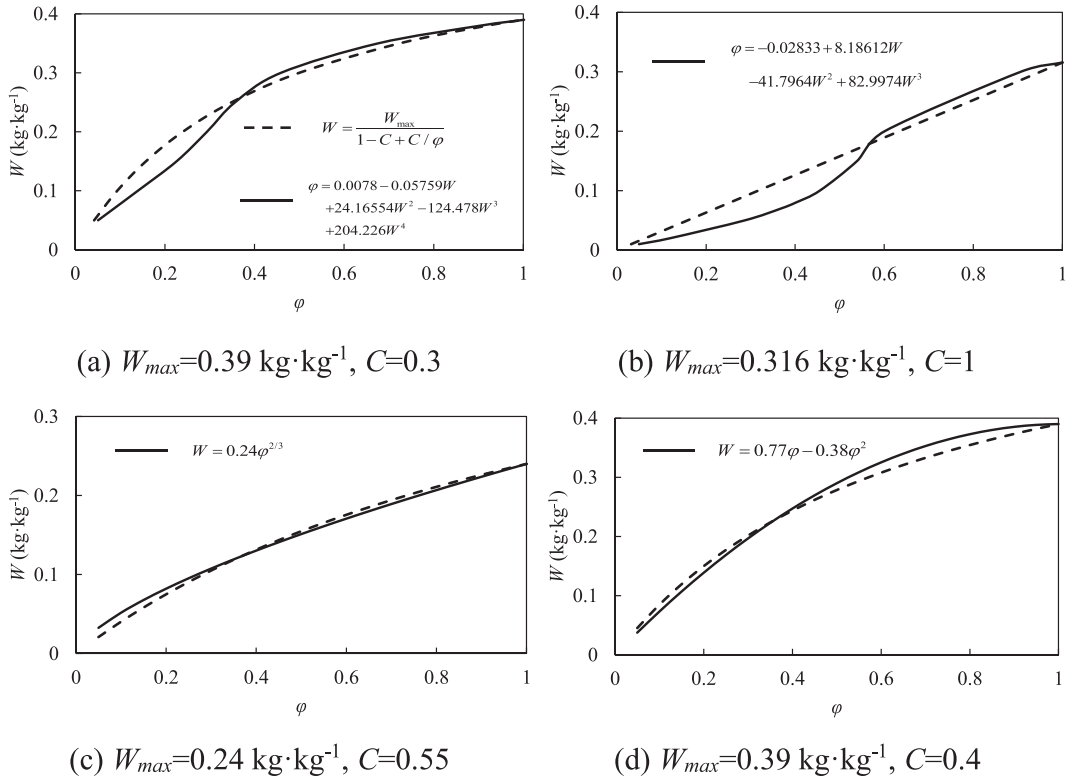


Fig. 1. Comparisons of the adsorption isotherm lines drawn from different equations with the universal adsorption isotherm equation.

erning equations: heat transfer, mass transfer, thermal balance and mass balance equations, shown as Eqs. (A1), (A2) and (A5), (A6) in Appendix A. The mathematical model, which is used for simulation analysis in the present paper, was developed based on the four governing equations and the details have been reported in previous papers (Tu et al., 2013b, 2014, 2016).

Apart from Eqs. (A1)–(A11) in Appendix A, equilibrium isotherms of desiccant materials are required to calculate equilibrium humidity ratio (ω_d) under specific temperature (t_d) and water capacity (W , defined as the mass of water adsorbed by 1 kg of dry adsorbent), with which mass transfer capacities between the air and the desiccant material can be calculated. Adsorption isotherm equations for silica-gel are summarized in Table 1, which connect W with equilibrium relative humidity (ϕ).

Eq. (1) is a common equilibrium isotherm equation for adsorption materials (Zhang, 2008):

$$W = \frac{W_{max}}{1 - C + C/\phi} \quad (1)$$

Shape factor (C) and maximum water capacity (W_{max}) are two parameters relating to adsorption properties of desiccant materials. The adsorption isotherms in Table 1 can be simplified as Eq. (1) with different C and W_{max} , as shown in Fig. 1.

Combining the adsorption isotherm equations and the Clapeyron equation shown in Eq. (2) (Zhang, 2008), the equilibrium hu-

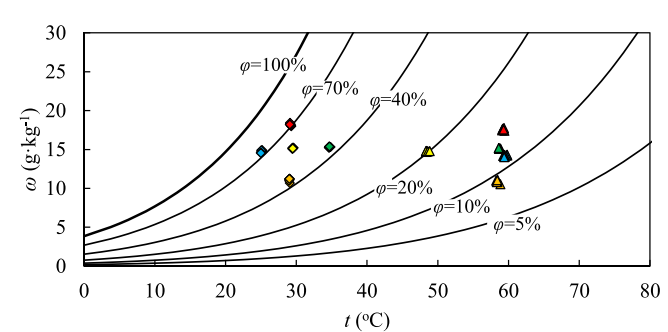


Fig. 2. Five groups of test conditions shown on the psychrometric chart.

Table 2

Parameters used in the model.

f	k_d kW m⁻¹ °C⁻¹	r_s kJ kg⁻¹	ρ_{ad} kg m⁻³	x	c_{pad} kJ kg⁻¹ °C⁻¹	Mol kg kmol⁻¹
0.1765	0.00022	$2.65 \cdot 10^3$	1129	0.7	0.92	18
σ	W_{max} Kg kg⁻¹	C	ρ_d kg m⁻³	a m	c_{pd} kJ kg⁻¹ °C⁻¹	d_h m
0.7	0.39	0.5	978	$11 \cdot 10^{-10}$	0.912	0.0012

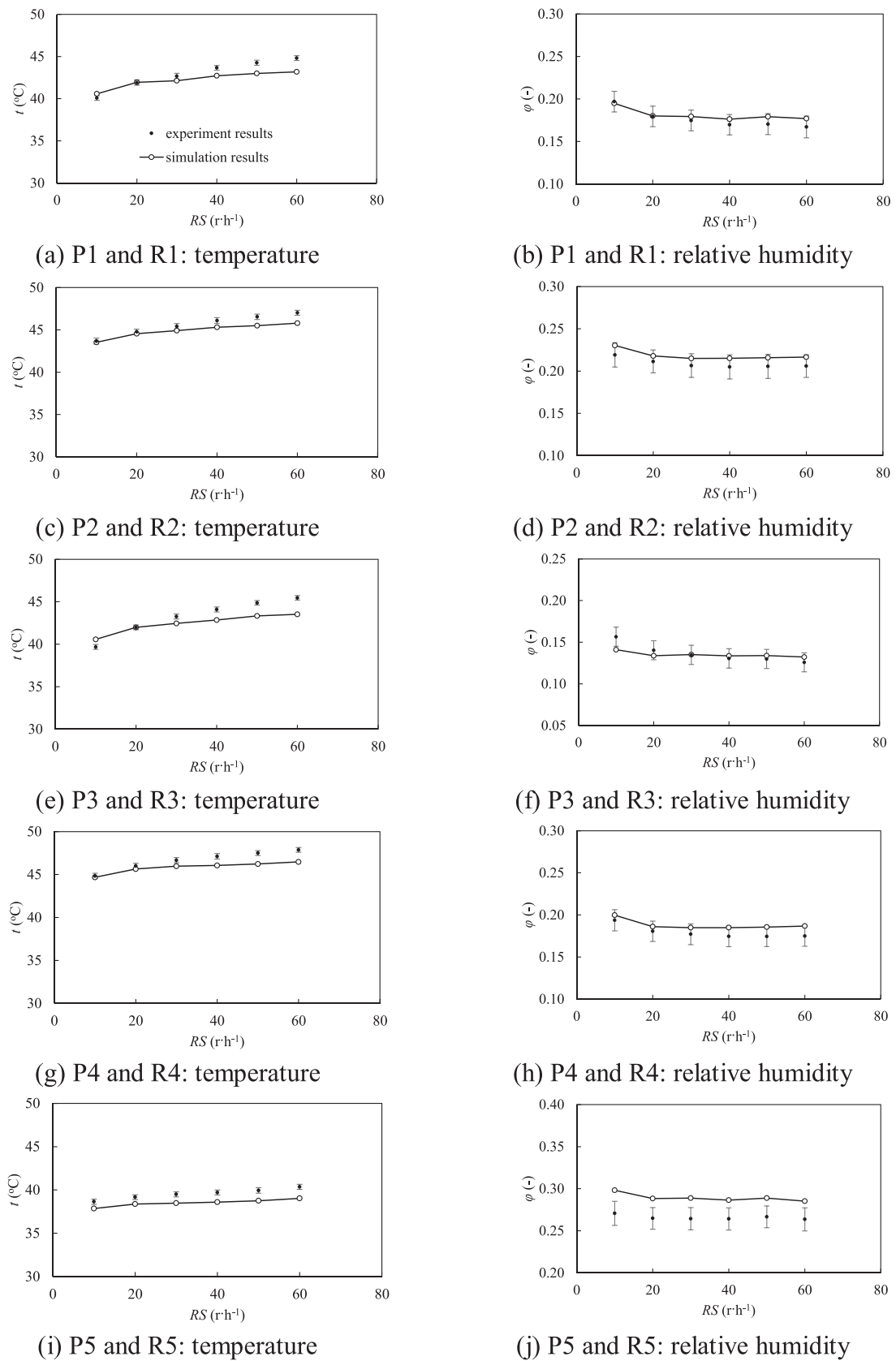


Fig. 3. Comparison of process air outlet temperature and relative humidity from experiment and simulation.

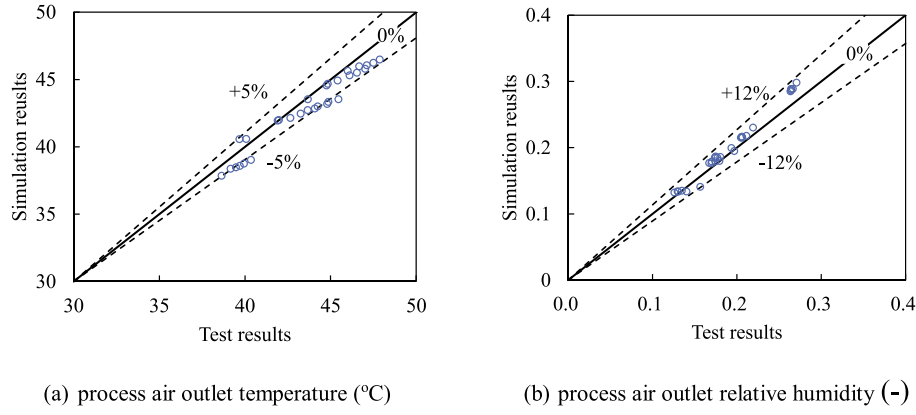


Fig. 4. Deviations between results from experiment and simulation.

midity ratio of the desiccant (ω_d), which is influenced by t_d and W/W_{max} , can be obtained, shown as Eq. (3):

$$\omega_d = \frac{\varphi}{10^{-6} \exp\left(\frac{5294}{t_d+273.15}\right) - 1.61\varphi} \quad (2)$$

$$\omega_d = \frac{W/W_{max}}{10^{-6} \exp\left(\frac{5294}{t_d+273.15}\right)\left(\frac{C-1}{C} + \frac{W}{W_{max}}\right) - 1.61\frac{W}{W_{max}}} \quad (3)$$

Eq. (3) is adopted in the mathematical model to investigate the effects of adsorption isotherm in the name of C and W_{max} on dehumidification performances of desiccant wheel systems.

2.2. Experiment validations of the desiccant wheel model

To validate the desiccant wheel model, field tests of a desiccant wheel were carried out. The test desiccant wheel was made of polymer. Four desiccant wheels with different length and radius were tested. The average height and width of the sinusoidal air channel were 1.28 mm and 2.83 mm, respectively. The cross section of the wheel was evenly divided between the process air and the regeneration air. And the two streams of air were designed to have the same mass flow rate, which was 0.1 kg s^{-1} . Under each working condition the outlet temperature and humidity ratio of the air were recorded for different rotational speeds. The experiment setup and results were detailed introduced in Cao et al.'s work (Cao et al., 2014).

Test results of one desiccant wheel under five groups of working conditions, which are shown in Fig. 2, were used for model validations. The diameter and length of the desiccant wheel are 150 mm and 175 mm, respectively. Parameters used in the mathematical model are listed in Table 2. The simulation results of process air outlet temperature and relative humidity changing with rotational speed under the five working conditions were compared with the corresponding experiment results. The detailed information can be referred to Fig. 3. The differences between the simulation results and the test results are shown in Fig. 4. It is demonstrated that the deviations of process air outlet temperature and relative humidity were within $\pm 5\%$ and $\pm 12\%$, respectively. Therefore, it was concluded that this mathematical model could predict the experiment results well. The following discussion were based on the simulation results of this model.

3. Air dehumidification at high and low relative humidity

In this section, dehumidification at high relative humidity and low relative humidity are discussed. Air handling processes of single stage and two-stage desiccant wheel dehumidification systems are investigated under mild- and humid-climates for regular and deep dehumidification applications, respectively.

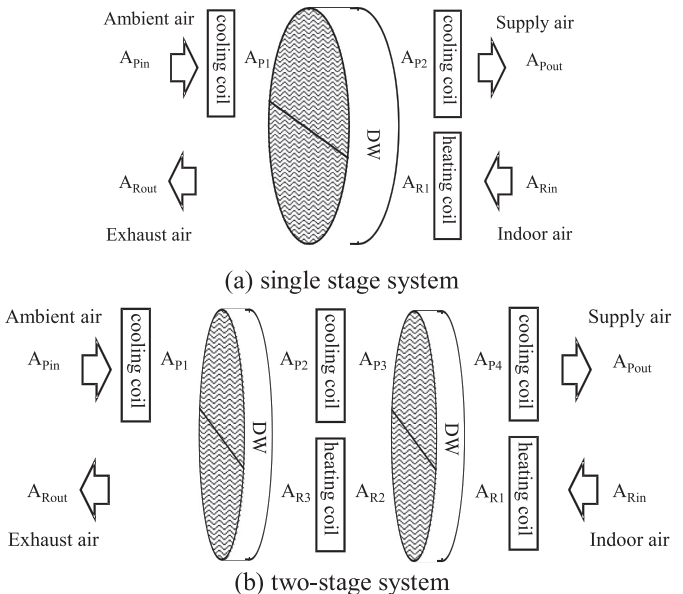


Fig. 5. Schematics of single stage and two-stage systems.

3.1. System description

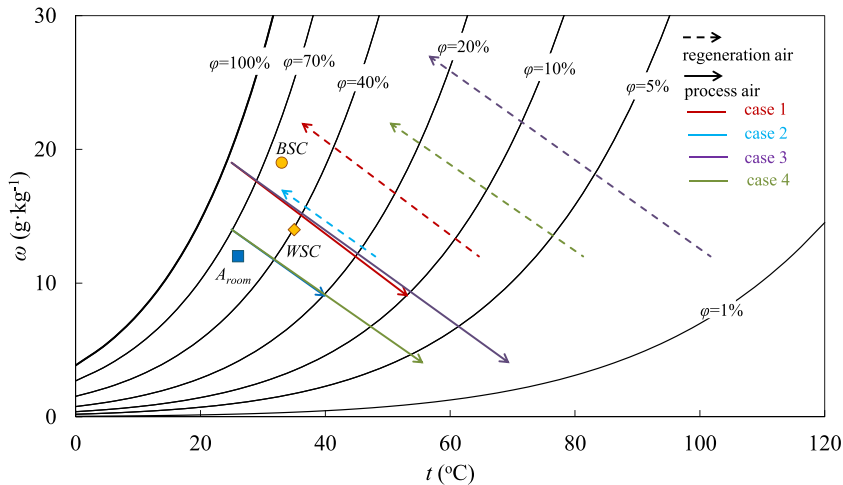
The single stage and two-stage desiccant wheel dehumidification systems are shown in Fig. 5. For both systems, the process air is cooled down by a cooling coil before entering the desiccant wheel. Similarly, the regeneration air is heated to the required regeneration temperature (t_{reg}) before regenerating the desiccant wheel. It should be emphasized that lower t_{reg} under the same working condition is beneficial for the adoption of low-grade heating sources such as solar energy and heat pump system, and smaller heating capacity of heat sources. Therefore, the following discussions are based on reducing t_{reg} .

The dimensions of desiccant wheels and working conditions for simulation studies are summarized in Table 3. Each desiccant wheel in the two-stage system has the same cross sectional area and half the thickness of the desiccant wheel in the single stage system. There are no physical models for cooling coils or heaters. The process air is cooled to t_c by each cooling coil. Similarly, the regeneration air is heated to the regeneration temperature (t_{reg}) by each heater. t_c is fixed at 25 °C in the following discussion. t_{reg} , which varies with working conditions, supply air humidity ratio, rotational speed, C and W_{max} , is to be determined through simulation. Beijing summer working condition (BSC: 33 °C, 19 g kg⁻¹),

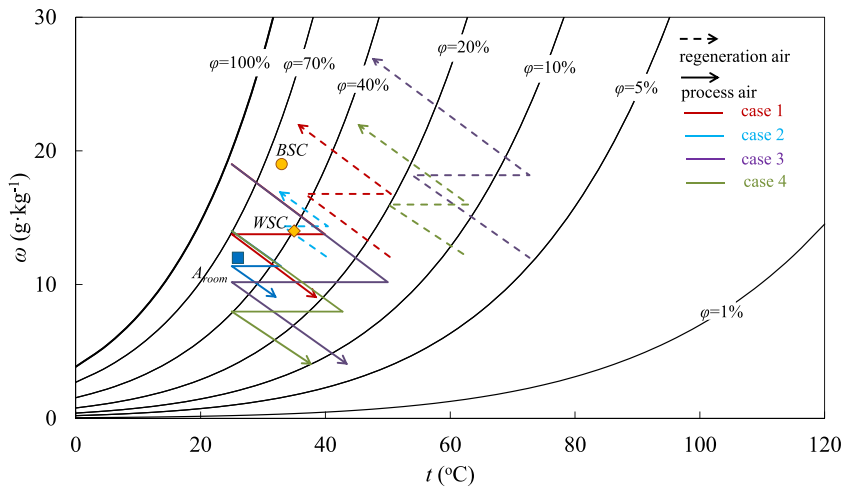
Table 3

Design conditions for the simulation analysis.

Working conditions	Desiccant wheel	Heat exchange coil
Process air volume flow rate: $2500 \text{ m}^3 \text{ h}^{-1}$	Radius: 0.5 m	Temperature after the cooling coils: $t_c = 25^\circ\text{C}$
BSC: $33^\circ\text{C}, 19 \text{ g kg}^{-1}$; WSC: $33^\circ\text{C}, 14 \text{ g kg}^{-1}$	Total thickness: 0.2 m	
Regeneration air: $2500 \text{ m}^3 \text{ h}^{-1}, 26^\circ\text{C}, 12 \text{ g kg}^{-1}$	Air path: 2 mm high and 2 mm wide	Temperature after the heating coils: t_{reg}
Supplied air for regular dehumidification: $2500 \text{ m}^3 \text{ h}^{-1}, 25^\circ\text{C}, 9 \text{ g kg}^{-1}$	$Nu: 2.463$	
Supplied air for deep dehumidification: $2500 \text{ m}^3 \text{ h}^{-1}, 25^\circ\text{C}, 4 \text{ g kg}^{-1}$		



(a) single stage system



(b) two-stage system

Fig. 6. Air handling processes for the four cases when $C = 0.3$, $W_{max} = 0.39 \text{ kg kg}^{-1}$ and $RS = 20 \text{ r h}^{-1}$.

which represents humid climate, and Washington airport summer working condition (WSC: $33^\circ\text{C}, 14 \text{ g kg}^{-1}$), which represents mild climate, are selected. 9 g kg^{-1} and 4 g kg^{-1} are selected as the supply air humidity ratio (humidity ratio of A_{Pout} in Fig. 5) representing regular and deep dehumidification, respectively.

3.2. Air handling processes of different cases

Four cases, which are regular dehumidification under BSC (case 1), regular dehumidification under WSC (case 2), deep dehumidification under BSC (case 3) and deep dehumidification under WSC (case 4), are discussed for the two systems.

The air handling processes (the cooling process from A_{Pin} to A_{P1} and the heating process from A_{Rin} to A_{R1} in Fig. 5 are not drawn on the psychrometric charts) for the above four cases of the single stage and two-stage systems are shown in Fig. 6. The corresponding regeneration temperature are shown in Fig. 7. These results are obtained based on parameters listed in Table 3. C and W_{max} are 0.3 and 0.39 kg kg^{-1} , respectively, representing silica-gel in Fig. 1(a). Rotational speed (RS) of the desiccant wheel are fixed at 20 r h^{-1} . It is illustrated by Fig. 6 that for the same system, the air is handled at a lower relative humidity range for the deep dehumidification (case 3 and case 4) as compared with the regular dehumidification (case 1 and case 2), and the corresponding t_{reg} is higher. For the same case, the air is handled at a higher

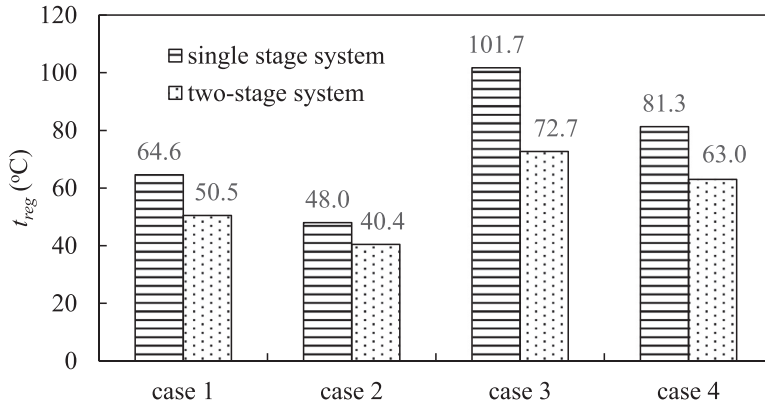


Fig. 7. t_{reg} of different scenarios when $C = 0.3$, $W_{max} = 0.39 \text{ kg kg}^{-1}$ and $RS = 20 \text{ r h}^{-1}$.

relative humidity in the two-stage system as compared with the single stage system, resulting in lower t_{reg} . t_{reg} varies from 40.4°C (case 2 of the two-stage system) to 101.7°C (case 3 of the single stage system). Fig. 7 shows that t_{reg} differences between the single stage and the two-stage systems range from 7.6°C (case 2) to 29°C (case 3).

The above discussions are based on fixed C , W_{max} and RS . In the next part, selections of C and W_{max} for high and low relative humidity dehumidification are analyzed with the aim of achieving relatively low t_{reg} . RS are taken into consideration and the following discussion is based on the optimal RS .

4. Effects of RS, C and W_{max} on t_{reg}

It is suggested that desiccant materials, of which C is smaller than 1, are suitable for dehumidification [2]. According to Fig. 1, C varies from 0.3 to 1, and W_{max} varies from 0.24 kg kg^{-1} to 0.4 kg kg^{-1} . In this section, cases with C equaling to 0.3, 0.5 and 1 are selected to cover adsorption materials in a wide range of C . W_{max} equaling to 0.3 kg kg^{-1} and 0.8 kg kg^{-1} are selected to represent adsorption material with regular and high water storage capacity. There are six combinations, which are $C = 0.1$ and $W_{max} = 0.3 \text{ kg kg}^{-1}$, $C = 0.1$ and $W_{max} = 0.8 \text{ kg kg}^{-1}$, $C = 0.3$ and $W_{max} = 0.3 \text{ kg kg}^{-1}$ and $C = 0.3$ and $W_{max} = 0.8 \text{ kg kg}^{-1}$, $C = 1$ and $W_{max} = 0.3 \text{ kg kg}^{-1}$ and $C = 1$ and $W_{max} = 0.8 \text{ kg kg}^{-1}$.

First, the effects of RS on t_{reg} are discussed. Next, the recommended C and W_{max} are discussed under the optimal RS (ORS). Finally, RS ranges which gives relatively low t_{reg} are analyzed.

4.1. Effects of RS on t_{reg}

The effects of RS on t_{reg} of single stage and two-stage systems under case 1 to case 4 are shown in Figs. 8–11. There are two things to be noticed. First, there are cross points among the t_{reg} - RS lines for the six groups' combinations of C and W_{max} in each figure. In other word, the preferred combination of C and W_{max} , which results in the lowest t_{reg} , differs with RS . Taking Fig. 8(a) as an example, when $RS = 10 \text{ r h}^{-1}$, the combination of $C = 0.3$ and $W_{max} = 0.8 \text{ kg kg}^{-1}$ results in the lowest t_{reg} . When $RS = 40 \text{ r h}^{-1}$, the combination of $C = 0.3$ and $W_{max} = 0.8 \text{ kg kg}^{-1}$ results in the highest t_{reg} and the combination of $C = 1$ and $W_{max} = 0.8 \text{ kg kg}^{-1}$ results in the lowest t_{reg} . Second, t_{reg} of the two-stage system may be higher than that of the single stage system if the RS is not properly selected. Taking Fig. 9 as an example, as for the combination of $C = 0.3$ and $W_{max} = 0.3 \text{ kg kg}^{-1}$ for case 2, when RS is 5 r h^{-1} , t_{reg} of the two-stage system (55°C) is slightly higher than that of the single stage system (54°C).

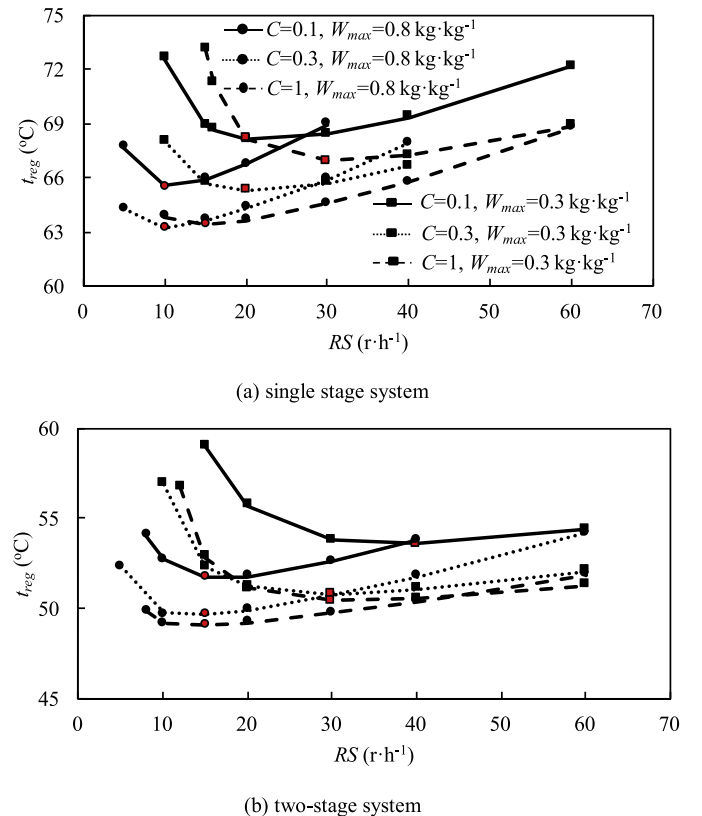


Fig. 8. Effects of C , W_{max} and RS on t_{reg} for case 1 of single stage and two-stage systems.

Based on the above two reasons, it is important to select the results at the ORS for discussion. It is demonstrated in Figs. 8–11 that an ORS exists for each scenario. When RS is away from the ORS, t_{reg} is increased compared with the one at the ORS. The ORS, shown as red dots in Figs. 8–11, for case 1 to case 4 are listed in Tables 4–7, respectively. The ORS differs with C and W_{max} , and is sensitive to W_{max} and ambient conditions. With the same supply air humidity ratio, larger W_{max} and less humid ambient conditions (WSC) lead to lower ORS.

This can be explained from Eq. (4):

$$ORS = \frac{3.6m_p \Delta\omega}{M_{DW} \Delta W} \quad (4)$$

Mass flow rate of the process air (m_p) and the mass of desiccant wheel (M_{DW}) are the same for each scenario. For the less

Table 4
Optimal RS, recommended range of RS and corresponding t_{reg} for case 1.

System	Single stage		Two-stage	
	ORS (range) (r h ⁻¹)	t_{reg} (range) (°C)	ORS (range) (r h ⁻¹)	t_{reg} (range) (°C)
$C = 0.1, W_{max} = 0.3 \text{ kg kg}^{-1}$	20 (15–40)	68.2 (68.2–69.3)	40 (30–60)	53.6 (53.6–54.4)
$C = 0.1, W_{max} = 0.8 \text{ kg kg}^{-1}$	10 (10–20)	65.6 (65.6–66.7)	15 (10–30)	51.8 (51.8–52.7)
$C = 0.3, W_{max} = 0.3 \text{ kg kg}^{-1}$	20 (15–30)	65.3 (65.3–65.7)	30 (20–40)	50.8 (50.8–51.2)
$C = 0.3, W_{max} = 0.8 \text{ kg kg}^{-1}$	10 (5–20)	63.3 (63.3–64.3)	15 (10–30)	49.7 (49.7–50.8)
$C = 1, W_{max} = 0.3 \text{ kg kg}^{-1}$	30 (20–40)	66.9 (66.9–68.1)	30 (20–60)	50.4 (50.4–51.3)
$C = 1, W_{max} = 0.8 \text{ kg kg}^{-1}$	15 (10–30)	63.4 (63.4–64.6)	15 (10–30)	49.1 (49.1–49.7)

Table 5
Optimal RS, recommended range of RS and corresponding t_{reg} for case 2.

System	Single stage		Two-stage	
	ORS (range) (r h ⁻¹)	t_{reg} (range) (°C)	ORS (range) (r h ⁻¹)	t_{reg} (range) (°C)
$C = 0.1, W_{max} = 0.3 \text{ kg kg}^{-1}$	20 (15–30)	49.8 (49.8–50.5)	30 (20–60)	42.3 (42.3–43.5)
$C = 0.1, W_{max} = 0.8 \text{ kg kg}^{-1}$	10 (5–15)	48.5 (48.5–49.2)	15 (10–30)	41.3 (41.3–42.6)
$C = 0.3, W_{max} = 0.3 \text{ kg kg}^{-1}$	15 (10–30)	47.8 (47.8–48.8)	20 (15–40)	40.7 (40.7–41.2)
$C = 0.3, W_{max} = 0.8 \text{ kg kg}^{-1}$	8 (5–15)	47.0 (47.0–47.8)	10 (5–20)	40.0 (40.0–40.8)
$C = 1, W_{max} = 0.3 \text{ kg kg}^{-1}$	15 (10–30)	47.7 (47.7–48.4)	20 (15–40)	40.2 (40.2–40.7)
$C = 1, W_{max} = 0.8 \text{ kg kg}^{-1}$	10 (5–20)	46.6 (46.6–47.5)	10 (5–30)	39.6 (39.6–40.6)

Table 6
Optimal RS, recommended range of RS and corresponding t_{reg} for case 3.

System	Single stage		Two-stage	
	ORS (range) (r h ⁻¹)	t_{reg} (range) (°C)	ORS (range) (r h ⁻¹)	t_{reg} (range) (°C)
$C = 0.1, W_{max} = 0.3 \text{ kg kg}^{-1}$	20 (15–20)	101.0 (101.0–101.8)	30 (20–40)	75.5 (75.5–76.8)
$C = 0.1, W_{max} = 0.8 \text{ kg kg}^{-1}$	8 (8–12)	95.9 (95.9–96.7)	15 (10–20)	72.7 (72.7–73.6)
$C = 0.3, W_{max} = 0.3 \text{ kg kg}^{-1}$	30 (25–30)	104.3 (104.3–105.3)	30 (25–40)	73.5 (73.5–74.2)
$C = 0.3, W_{max} = 0.8 \text{ kg kg}^{-1}$	12 (10–20)	96.0 (96.0–97.1)	15 (10–20)	70.7 (70.7–71.3)
$C = 1, W_{max} = 0.3 \text{ kg kg}^{-1}$			48 (40–60)	77.7 (77.7–78.6)
$C = 1, W_{max} = 0.8 \text{ kg kg}^{-1}$	30 (25–30)	104.4 (104.4–105.5)	25 (20–30)	71.7 (71.7–72.1)

Table 7
Optimal RS, recommended range of RS and corresponding t_{reg} for case 4.

System	Single stage		Two-stage	
	ORS (range) (r h ⁻¹)	t_{reg} (range) (°C)	ORS (range) (r h ⁻¹)	t_{reg} (range) (°C)
$C = 0.1, W_{max} = 0.3 \text{ kg kg}^{-1}$	15 (12–20)	82.2 (82.2–83.2)	20 (20–30)	65.5 (65.5–65.7)
$C = 0.1, W_{max} = 0.8 \text{ kg kg}^{-1}$	5 (5–10)	79.5 (79.5–80.4)	10 (8–15)	63.3 (63.3–63.9)
$C = 0.3, W_{max} = 0.3 \text{ kg kg}^{-1}$	20 (15–25)	82.1 (82.1–82.8)	20 (15–30)	63.8 (63.8–65.1)
$C = 0.3, W_{max} = 0.8 \text{ kg kg}^{-1}$	8 (8–15)	78.3 (78.3–80.0)	10 (8–15)	61.7 (61.7–62.2)
$C = 1, W_{max} = 0.3 \text{ kg kg}^{-1}$	40	91.9	40 (30–50)	65.5 (65.5–66.3)
$C = 1, W_{max} = 0.8 \text{ kg kg}^{-1}$	20 (15–20)	81.8 (81.8–81.2)	15 (15–30)	62.2 (62.2–63.4)

humid ambient condition, the dehumidification capacity ($\Delta\omega$) is lower. ΔW is the average water capacity change during dehumidification process. Desiccant material with higher W_{max} can absorb more water to reach its limit and ΔW can be higher. The above two reasons explain why ORS is lower at larger W_{max} and less humid ambient conditions.

It can also be observed from Figs. 8–11 that when RS is close to ORS, t_{reg} does not change much. The ranges of RS with t_{reg} variation within 1 °C around the lowest t_{reg} are listed in Tables 4–7. This is more applicable for real application. The recommended RS ranges of single stage and two-stage systems for the regular dehumidification (case 1 and case 2) and deep dehumidification (case 3 and case 4) are demonstrated in Figs. 12 and 13. Similar with the optimal rotational speed, Higher W_{max} leads to lower RS ranges when other conditions are the same.

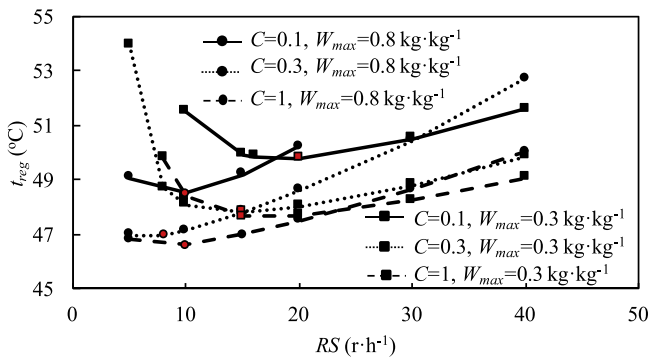
4.2. Suggested C and W_{max} and the recommended RS ranges

t_{reg} under ORS or recommended rotational speed ranges are listed in Tables 4–7 for different combinations of C and W_{max} for the single stage and two-stage systems under different cases. It is

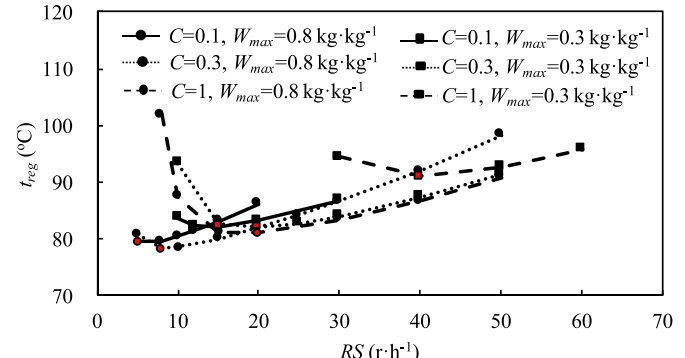
common for the four cases that for both single stage and two-stage systems, t_{reg} is lower when adsorption materials with larger W_{max} is adopted. Larger W_{max} is recommended especially for dehumidification at lower relative humidity, such as the single stage system, humid ambient conditions and deep dehumidification.

C has different effects on t_{reg} between the regular dehumidification and deep dehumidification cases. For the regular dehumidification cases (case 1 and case 2), larger C ($C = 1$) is recommended while smaller C ($C = 0.3$) is preferred for the deep dehumidification cases (case 3 and case 4). For regular dehumidification of the single stage system operated under case 1, shown in Table 4, the effects of C on t_{reg} are minor when W_{max} is large (0.8 kg kg⁻¹). And $C = 0.3$ and $C = 1$ are both preferred. For deep dehumidification of the single stage system operated under case 3, shown in Table 6, t_{reg} of the scenario when $C = 0.1$ is slightly lower than that of $C = 0.3$ when W_{max} is large (0.8 kg kg⁻¹). However, the difference is so small that $C = 0.1$ and $C = 0.3$ are both preferred.

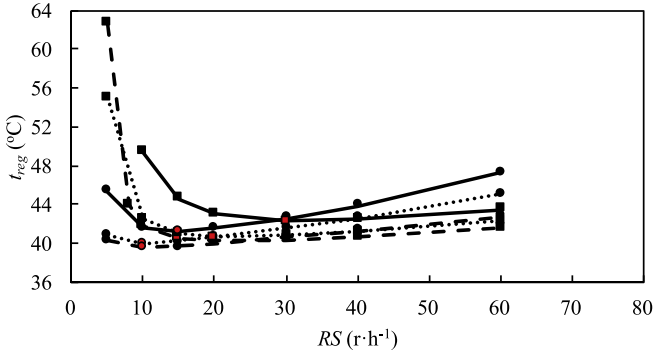
It is concluded that for dehumidification at high relative humidity ranges with low t_{reg} , i.e. two-stage system and less humid ambient condition for regular dehumidification, adsorption materials with C closer to 1 are recommended. For dehumidifica-



(a) single stage system

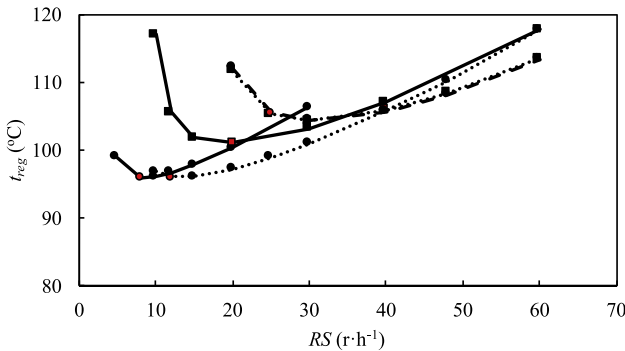


(a) single stage system

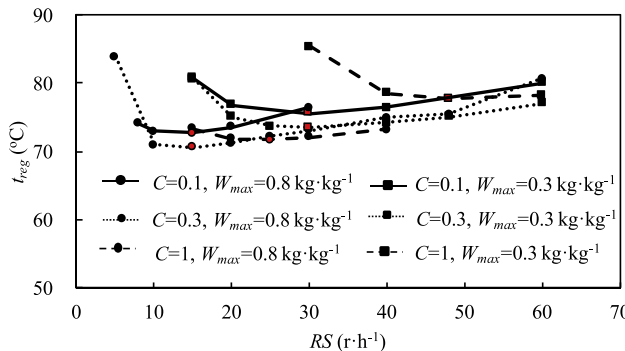


(b) two-stage system

Fig. 9. Effects of C , W_{max} and RS on t_{reg} for case 2 of single stage and two-stage systems.

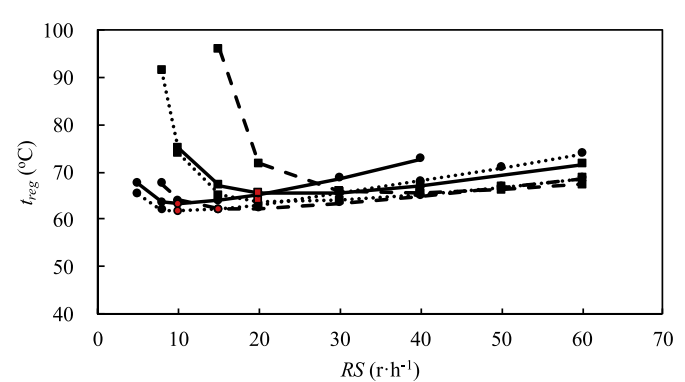


(a) single stage system (results of $C=1$ and $W_{max}=0.3$ kg·kg $^{-1}$ are not shown in this figure)



(b) two-stage system

Fig. 10. Effects of C , W_{max} and RS on t_{reg} for case 3 of single stage and two-stage systems.



(a) single stage system

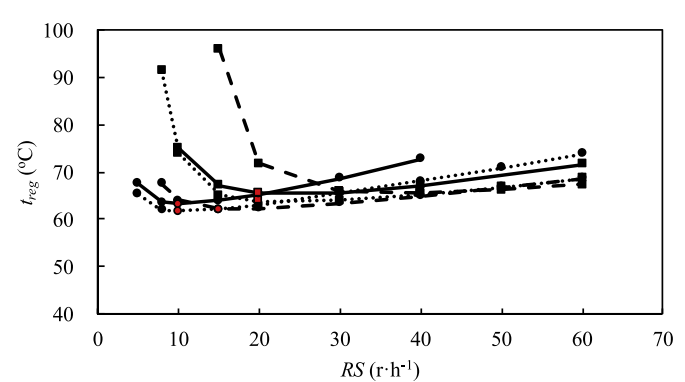


Fig. 11. Effects of C , W_{max} and RS on t_{reg} for case 4 of single stage and two-stage systems.

tion at low relative humidity ranges with high t_{reg} , i.e. deep dehumidification, smaller C is preferred. The recommended C , W_{max} and RS ranges for different cases of the single stage and two-stage systems are listed in Table 8. For regular dehumidification, $C = 1$ and $W_{max} = 0.8 \text{ kg kg}^{-1}$ are recommended for the single stage and two-stage systems under a wide range of working conditions (BSC and WSC). Whereas, for deep dehumidification $C = 0.3$ and $W_{max} = 0.8 \text{ kg kg}^{-1}$ are preferred for the single stage and two-stage systems under a wide range of working conditions. The recommended RS ranges of the single stage and two-stage systems under BSC and WSC for regular and deep dehumidification applications are listed in Table 8. The RS ranges of 10–15 r h $^{-1}$ works for the regular and deep dehumidification of the single stage and two-stage system under a wide range of working conditions.

5. Discussions

The previous analysis shows different requirements of shape factor (C) for dehumidification at low relative humidity range and high relative humidity range, or, in other words, regular dehumidification and deep dehumidification. The recommended RS ranges shown in Table 8 are proposed based on a fixed air flow rate, thickness of desiccant wheel and W_{max} . The reasons for the effects of shape factors (C) are theoretically discussed in this section. And the effects of wheel thickness and W_{max} on the recommended RS ranges are analyzed afterwards.

Table 8Recommended range of RS, C and W_{max} .

	BSC	WSC	BSC and WSC	Single- and two-stage systems	Regular and deep dehumidification
Regular dehumidification: $C = 1$, $W_{max} = 0.8 \text{ kg kg}^{-1}$	Single stage 10–30 r h ⁻¹ Two-stage 10–30 r h ⁻¹	5–20 r h ⁻¹ 5–30 r h ⁻¹	10–20 r h ⁻¹ 10–30 r h ⁻¹	10–20 r h ⁻¹	10–15 r h ⁻¹
Deep dehumidification: $C = 0.3$, $W_{max} = 0.8 \text{ kg kg}^{-1}$	Single stage 10–20 r h ⁻¹ Two-stage 10–20 r h ⁻¹	8–15 r h ⁻¹ 8–15 r h ⁻¹	10–15 r h ⁻¹ 10–15 r h ⁻¹	10–15 r h ⁻¹	10–15 r h ⁻¹

5.1. Theoretical analysis of the effects of C for different dehumidification applications

It is shown in Eq. (3) that ω_d is influenced by t_d , C and W/W_{max} . Fig. 14 shows the relations of ω_d and t_d at the same W/W_{max} , which is called the iso W/W_{max} lines, on the psychrometric chart. When C equals to 1, the iso W/W_{max} lines of desiccant material overlap the iso-relative humidity lines of the air with the same value. The iso W/W_{max} lines of the same value are greatly different among adsorption materials with different C.

The effects of C on the performances of solid desiccant dehumidification can be analyzed through $\partial\omega_d/\partial C$ and $\partial t_d/\partial C$, expressed as Eqs. (5) and (6), respectively:

$$\frac{\partial\omega_d}{\partial C} = \frac{\partial\omega_d}{\partial\phi_d} \cdot \frac{\partial\phi_d}{\partial C} \quad (5)$$

$$\frac{\partial t_d}{\partial C} = \frac{\partial t_d}{\partial\phi_d} \cdot \frac{\partial\phi_d}{\partial C} \quad (6)$$

According to Eq. (2), $\partial\omega_d/\partial\phi_d$ and $\partial t_d/\partial\omega_d$ can be written as Eqs. (7) and (8), respectively:

$$\frac{\partial\omega_d}{\partial\phi_d} = \frac{\omega_d}{\phi_d} (1 + 1.61\omega_d) \quad (7)$$

$$\frac{\partial t_d}{\partial\phi_d} = \frac{(t_d + 273.15)^2}{5294\phi_d} \quad (8)$$

According to Eq. (1), $\partial\phi_d/\partial C$ can be written as Eq. (9):

$$\frac{\partial\phi_d}{\partial C} = \frac{\phi_d(1 - \phi_d)}{C} \quad (9)$$

Combining Eqs. (7)–(9), Eqs. (5)–(6) are expressed as Eqs. (10)–(11), respectively:

$$\frac{\partial\omega_d}{\partial C} = \frac{\omega_d(1 + 1.61\omega_d)(1 - \phi_d)}{C} \quad (10)$$

$$\frac{\partial t_d}{\partial C} = \frac{(1 - \phi_d)(t_d + 273.15)^2}{5294C} \quad (11)$$

According to Eqs. (10) and (11), $\partial\omega_d/\partial C$ is positive and $\partial t_d/\partial C$ is negative. This means that when t_d and W/W_{max} are fixed, ω_d is higher of desiccant material with higher C. In other word, to get the same ω_d at the same W/W_{max} , temperature of desiccant material with higher C is lower, which is beneficial for the regeneration process. However, this has negative effects on the dehumidification process for higher ω_d of desiccant material with higher C at the same W/W_{max} and t_d . Therefore, when the inlet temperature and humidity ratio of the process air are fixed as discussed in this paper, to reach the same supply air humidity ratio, W/W_{max} of desiccant material with higher C should be lower. It is illustrated in Fig. 14 that t_d increases with the reduction of W/W_{max} at the fixed ω_d and C. Because of lower W/W_{max} ranges especially for single stage and deep dehumidification scenarios, t_{reg} , which is the inlet temperature of the regeneration air, may be increased when desiccant material with higher C is adopted.

Taking single stage system as an example, the states of desiccant materials when C = 1 and C = 0.3 ($W_{max} = 0.8 \text{ kg kg}^{-1}$) under BSC for deep dehumidification application and WSC for regular dehumidification application are shown in Figs. 15 and 16, respectively. Fig. 15 is the results of BSC for deep dehumidification application. It shows that the relative humidity of supply air is close to 1%. The angle average W/W_{max} of desiccant material along the wheel thickness direction is from 6% to 78% when C = 0.3, while it is from 1% to 35% when C = 1. For low relative humidity dehumidification, the negative effects of low W/W_{max} of higher C (W/W_{max} is 1% when C = 1) dominates, resulting in higher t_{reg} (104.4 °C) as compared with the scenario when C = 0.3.

Fig. 16 is the results of WSC for regular dehumidification application. It shows that the relative humidity of supply air is close to 15%. Similar with BSC for the deep dehumidification application, the angle average W/W_{max} of desiccant material along the wheel thickness direction when C = 0.3, which is from 43% to 62%, is higher than those when C = 1, which is from 15% to 49%. However, for dehumidification at high relative humidity ranges, the advantages of lower t_d at the same W/W_{max} and ω_d of higher C (C = 1) outstands, especially at higher W/W_{max} , resulting in lower t_{reg} (46.6 °C) as compared with the scenario when C = 0.3.

5.2. Influencing factors of the recommended RS ranges

The recommended RS ranges in the previous discussions are based on the fixed air flow rate, desiccant wheel thickness and radius, and W_{max} . From the mass balance equation shown in Eq. (12), RS can be expressed as Eq. (13).

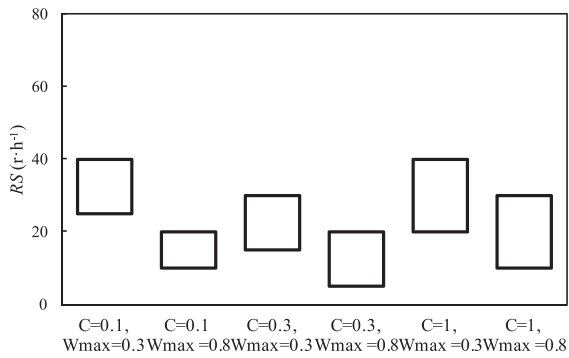
$$G_a\rho_a\Delta\omega = RS \cdot \pi R^2 L \rho_{ad} \Delta W \quad (12)$$

$$RS \left(\frac{\Delta W}{W_{max}} \frac{1}{\Delta\omega} \right) = \frac{G_a\rho_a}{\pi R^2 L \rho_{ad} W_{max}} = \frac{u_a \rho_a}{2\rho_{ad} L W_{max}} \quad (13)$$

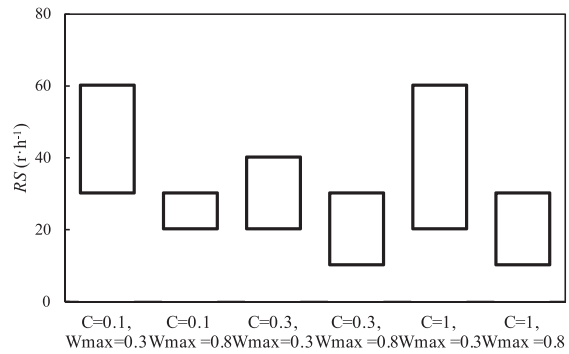
where $\Delta\omega$ is the humidity ratio differences between the inlet and outlet process air; ΔW is the average water capacity change of the desiccant material leaving and entering the dehumidification region; u_a is the air velocity and L is the wheel thickness. Normally u_a should be in an appropriate range to guarantee a satisfying heat and mass transfer coefficient, which is fixed at 1.77 m s⁻¹ in the discussion. $\Delta\omega$ is the task to be accomplished. Therefore, the optimal RS is related to L and W_{max} .

It is shown in Table 8 that there exist overlaps of recommended RS between deep dehumidification and regular dehumidification. According to Table 8, the universal recommended RS range, which is 10–15 r h⁻¹ when L = 0.2 m and $W_{max} = 0.8 \text{ kg kg}^{-1}$, is the same with the results of two-stage system under BSC and WSC for deep dehumidification. In this subsection, the effects of L and W_{max} on the recommended RS ranges are discussed based on the two-stage system under BSC and WSC for deep dehumidification application. C is 0.3 for the following discussion.

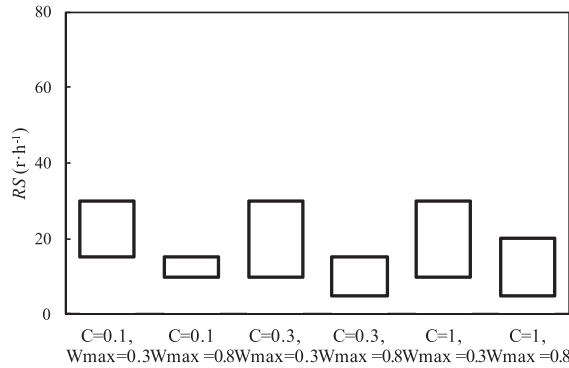
L equaling to 0.1 m and 0.3 m are selected for discussion when $W_{max} = 0.8 \text{ kg kg}^{-1}$. The variations of t_{reg} with RS under BSC and WSC when L = 0.1 m and 0.3 m are shown in Fig. 17. The optimal RS, recommended RS ranges and the corresponding t_{reg} are



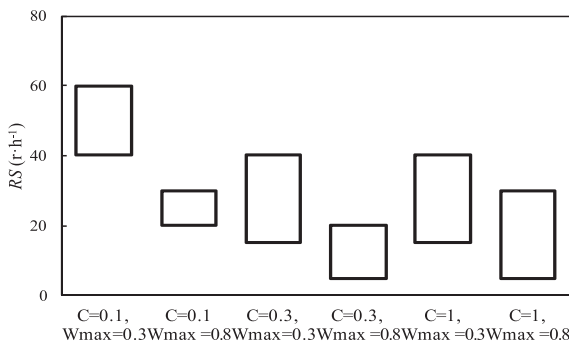
(a) case 1: single stage system



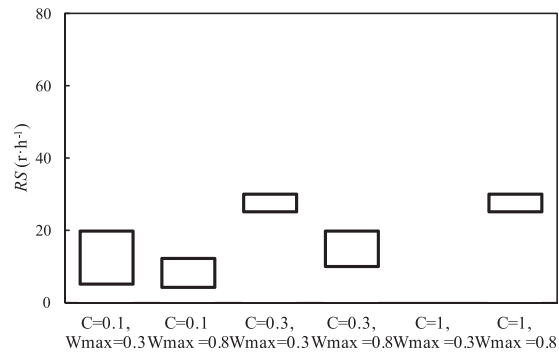
(b) case 1: two-stage system



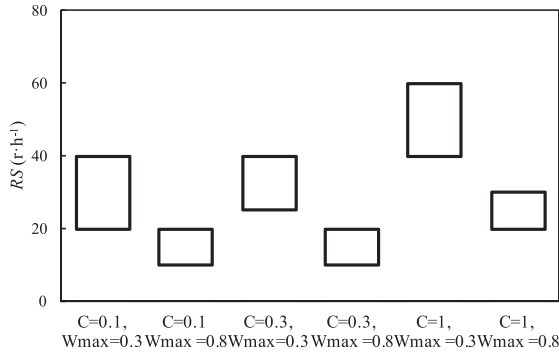
(c) case 2: single stage system



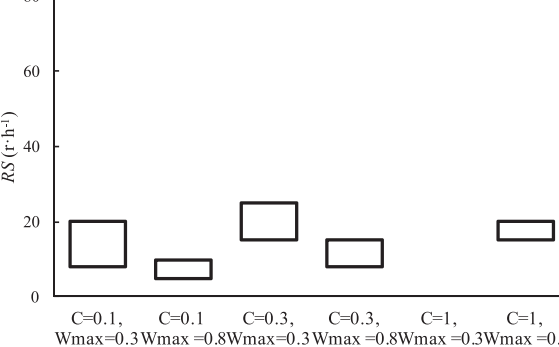
(d) case 2: two-stage system

Fig. 12. Recommended rotational speed ranges for regular dehumidification regarding single stage and two-stage systems under different combinations of C and W_{max} .

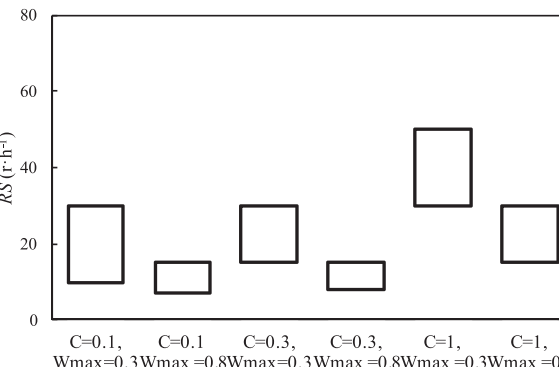
(a) case 3: single stage system



(b) case 3: two-stage system



(c) case 4: single stage system



(d) case 4: two-stage system

Fig. 13. Recommended rotation speed ranges for deep dehumidification regarding single stage and two-stage systems under different combinations of C and W_{max} .

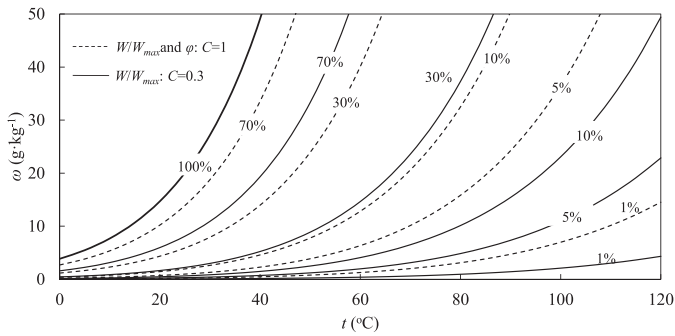
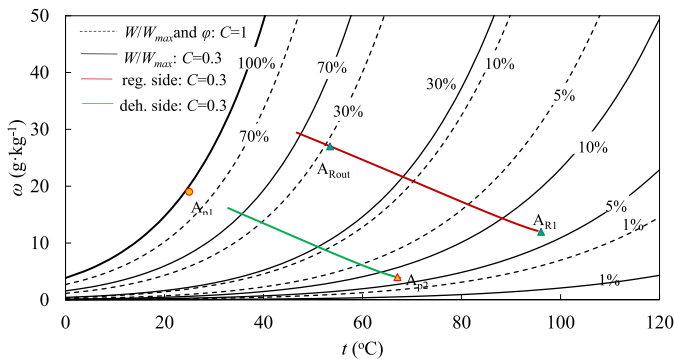
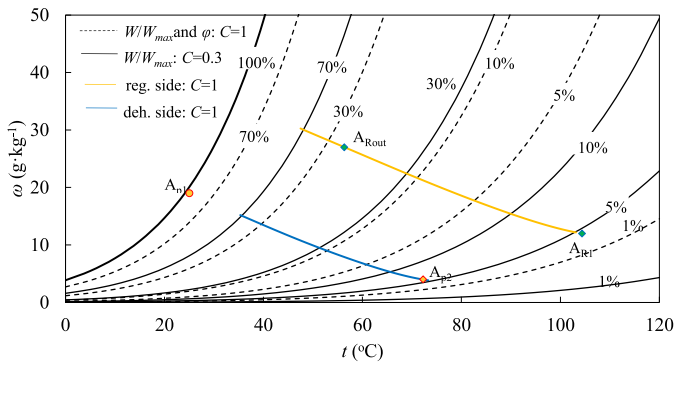


Fig. 14. Iso W/W_{max} lines of desiccant materials on the psychrometric chart when C equals to 1 and 0.3.



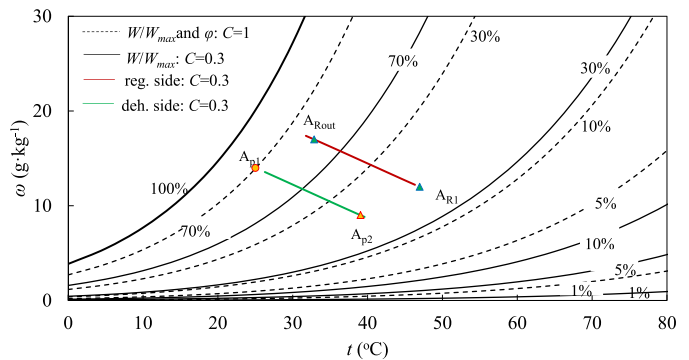
(a) $C=0.3$ and $W_{max}=0.8 \text{ kg} \cdot \text{kg}^{-1}$



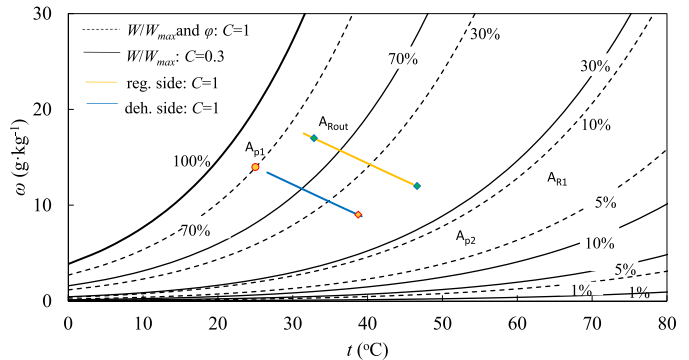
(b) $C=1$ and $W_{max}=0.8 \text{ kg} \cdot \text{kg}^{-1}$

Fig. 15. Angle average state of desiccant material at the dehumidification side and regeneration side along the wheel thickness direction: BSC for deep dehumidification application.

listed in Table 9. The results show that under the optimal RS, the increase of L is beneficial for the reduction of t_{reg} . Taking the deep dehumidification of the two-stage system as an example, when L increases from 0.1 m to 0.2 m, t_{reg} reduces from 83.1 °C to 70.7 °C under BSC. However, the improvement rate slows down as further increase of L , with a reduction of around 4 °C when L increased from 0.2 m to 0.3 m. As discussed in Section 4, the recommended RS ranges, which is for high or low relative humidity dehumidification of single and two-stage system under a wide range of working conditions, is 10–15 r h⁻¹ when $L = 0.2$ m. When $L = 0.1$ m, the recommended RS range is 20–30 r h⁻¹, which is half the results of $L = 0.2$ m. When $L = 0.3$ m, the recommended RS range is 6–10 r h⁻¹, which is around 1/3 the results of $L = 0.1$ m. Therefore, RS• L can be regarded as constant. According to Eq. (13),



(a) $C=0.3$ and $W_{max}=0.8 \text{ kg} \cdot \text{kg}^{-1}$



(b) $C=1$ and $W_{max}=0.8 \text{ kg} \cdot \text{kg}^{-1}$

Fig. 16. Angle average state of desiccant material at the dehumidification side and regeneration side along the wheel thickness direction: WSC for regular dehumidification application.

Table 9

Recommended RS range for desiccant wheels with different thickness ($C = 0.3$, $W_{max} = 0.8 \text{ kg} \cdot \text{kg}^{-1}$).

L (m)	Working condition	ORS (range) (r h ⁻¹)	t_{reg} (range) (°C)	Recommended RS range (r h ⁻¹)
0.1	BSC	25 (20–40)	83.1 (83.1–84.0)	20–30
	WSC	20 (15–30)	70.2 (70.2–70.8)	
0.2	BSC	15 (10–20)	70.7 (70.7–71.3)	10–15
	WSC	10 (8–15)	61.7 (61.7–62.2)	
0.3	BSC	8 (6–15)	66.8 (66.8–67.9)	6–10
	WSC	8 (5–10)	59.3 (59.3–59.6)	

Table 10

Recommended RS range for desiccant material with different W_{max} ($C = 0.3$, $L = 0.2$ m).

W_{max} (kg kg ⁻¹)	Working condition	ORS (range) (r h ⁻¹)	t_{reg} (range) (°C)	Recommended RS range (r h ⁻¹)
0.3	BSC	30 (25–40)	73.5 (73.5–74.2)	25–30
	WSC	20 (15–30)	63.8 (63.8–65.1)	
0.5	BSC	20 (15–30)	71.7 (71.7–72.5)	15–25
	WSC	15 (10–25)	62.4 (62.4–63.4)	
0.8	BSC	15 (10–20)	70.7 (70.7–71.3)	10–15
	WSC	10 (8–15)	61.7 (61.7–62.2)	

$(\Delta W/W_{max})/\Delta \omega$ under the optimal cases is almost the same under different L .

W_{max} equaling to 0.3 kg kg⁻¹, 0.5 kg kg⁻¹ and 0.8 kg kg⁻¹ are selected for discussion and L is fixed at 0.2 m. The recommended RS ranges for different W_{max} are shown in Table 10. It shows that larger W_{max} results in lower RS ranges and lower t_{reg} . The results

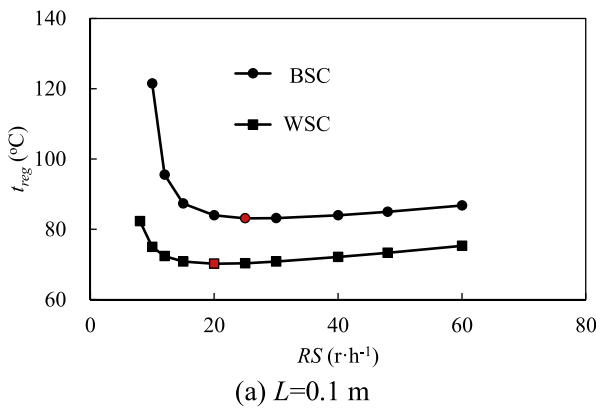
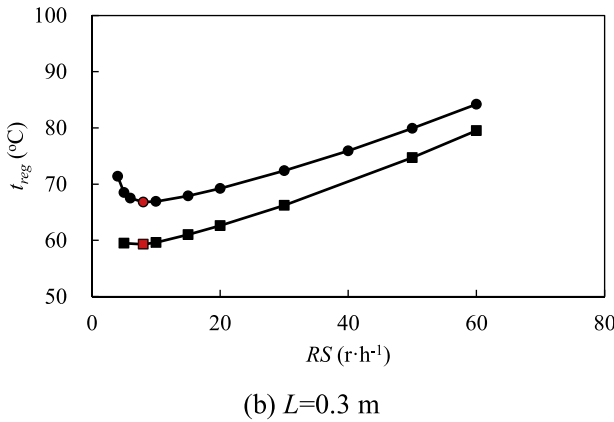
(a) $L=0.1\text{ m}$ 

Fig. 17. Variation of t_{reg} with RS for different wheel thickness: deep dehumidification of the two-stage system ($C = 0.3$ and $W_{max} = 0.8 \text{ kg kg}^{-1}$).

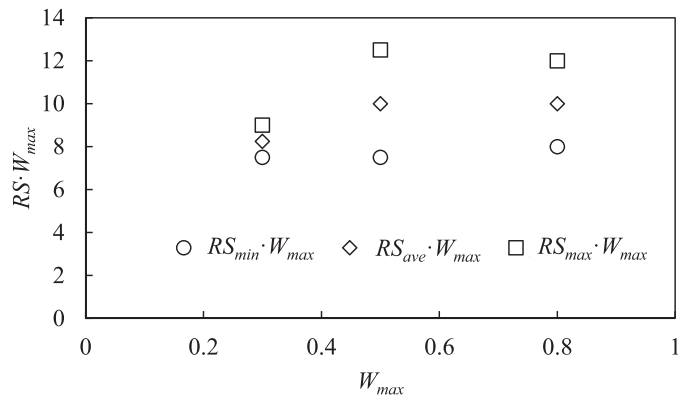


Fig. 18. W_{max} multiplying the maximum, average and minimum values of each RS ranges for different W_{max} .

of $RS_{max} \cdot W_{max}$, $RS_{ave} \cdot W_{max}$ and $RS_{min} \cdot W_{max}$ are shown in Fig. 18. It shows that $RS \cdot W_{max}$ can be regarded as constant under different W_{max} . According to Eq. (13), $(\Delta W/W_{max})/\Delta\omega$ under the optimal cases is almost the same.

Since $(\Delta W/W_{max})/\Delta\omega$ under the optimal cases is almost the same for different L and W_{max} , $RS \cdot L \cdot W_{max}$ can be regarded as a constant. ORS or optimal RS range for desiccant wheels with different L and desiccant materials with different W_{max} can be calculated accordingly. For desiccant wheels discussed in this paper, the density of adsorption material is 1129 kg m^{-3} , and it takes 70% of the wheel's volume. The wheel's facial area is evenly divided between the process air and the regeneration air with the facial air velocity being around 1.77 m s^{-1} . The recommended RS is $25\text{--}30 \text{ r h}^{-1}$ when $W_{max} = 0.3 \text{ kg kg}^{-1}$ and $L = 0.2 \text{ m}$. Based on this, recom-

Table 11
Recommended RS range for desiccant material with different W_{max} and L .

	Recommended RS ranges	Total wheel thickness in the system (m)		
		0.1 m	0.2 m	0.3 m
W_{max}				
0.3 kg kg^{-1}	$0.3\text{--}60 \text{ r h}^{-1}$	$25\text{--}30 \text{ r h}^{-1}$	$17\text{--}20 \text{ r h}^{-1}$	
0.4 kg kg^{-1}	$38\text{--}45 \text{ r h}^{-1}$	$19\text{--}23 \text{ r h}^{-1}$	$13\text{--}15 \text{ r h}^{-1}$	
0.5 kg kg^{-1}	$30\text{--}36 \text{ r h}^{-1}$	$15\text{--}18 \text{ r h}^{-1}$	$10\text{--}12 \text{ r h}^{-1}$	
0.6 kg kg^{-1}	$25\text{--}30 \text{ r h}^{-1}$	$13\text{--}15 \text{ r h}^{-1}$	$8\text{--}10 \text{ r h}^{-1}$	
0.8 kg kg^{-1}	$19\text{--}23 \text{ r h}^{-1}$	$9\text{--}11 \text{ r h}^{-1}$	$6\text{--}8 \text{ r h}^{-1}$	

mended RS ranges for desiccant material with different W_{max} and desiccant wheels with different L are listed in Table 11.

5.3. Case studies

In this subsection, performances of the system shown in Fig. 5(a), which is used to process ambient air ($2500 \text{ m}^3 \text{ h}^{-1}$, 33°C , 19 g kg^{-1}) and regenerated by the indoor air ($2500 \text{ m}^3 \text{ h}^{-1}$, 26°C , 12 g kg^{-1}), operated under the above recommended parameters are discussed. The supply air humidity ratio is 9 g kg^{-1} . The structure of the desiccant wheel is the same as Table 3 except that the thickness is 0.15 m . According to the above analysis, the recommended parameters are: $C = 0.3$, $W_{max} = 0.8 \text{ kg kg}^{-1}$, $RS = 15 \text{ r h}^{-1}$. Another group of parameters of $C = 0.1$, $W_{max} = 0.3 \text{ kg kg}^{-1}$ and $RS = 10 \text{ r h}^{-1}$ is selected to evaluate performance improvement.

Under the recommended parameters, namely $C = 0.3$, $W_{max} = 0.8 \text{ kg kg}^{-1}$, $RS = 15 \text{ r h}^{-1}$, t_{reg} is 65.7°C . When C is changed to 0.1 , t_{reg} is increased to 68.0°C . When C is changed to 0.1 and W_{max} is changed to 0.3 kg kg^{-1} , t_{reg} is increased to 73.6°C . When C is changed to 0.1 and W_{max} is changed to 0.3 kg kg^{-1} and RS is changed to 10 r h^{-1} , t_{reg} is increased to 82.6°C . The increase of t_{reg} will increase heating capacity of heating sources, affect adoption of low-grade heat sources and reduce system performances.

6. Conclusions

This paper aims to suggest the proper adsorption isotherms from the aspects of shape factor (C) and maximum water capacity (W_{max}), as well as rotational speed (RS) ranges, for high and low relative humidity dehumidification applications to achieve low temperature regeneration (t_{reg}). The performances of single stage and two-stage desiccant wheel systems under mild (WSC: 33°C and 14 g kg^{-1}) and humid (BSC: 33°C and 19 g kg^{-1}) working conditions for regular (supply air: 9 g kg^{-1}) and deep dehumidification (supply air: 4 g kg^{-1}) applications were analyzed through simulation. The mathematical model was validated by the experiment results. The main conclusions are as follows:

- Compared with the regular dehumidification, the air is handled at a lower relative humidity range for the deep dehumidification and the corresponding t_{reg} is higher. For the same working condition and supply air humidity ratio, the air is handled at a higher relative humidity for the two-stage system as compared with the single stage system, resulting in lower t_{reg} .
- The proper C and W_{max} are suggested under the optimal rotational speed. Large W_{max} is preferred to reduce t_{reg} especially for deep dehumidification of the single-stage system under humid climate. For dehumidification at high relative humidity ratio ranges with low t_{reg} , adsorption materials with C equaling to 1 are preferred. $C = 1$ and $W_{max} = 0.8 \text{ kg kg}^{-1}$ is recommended for the single stage and two-stage systems for regular dehumidification. Whereas, for dehumidification at low relative

humidity ranges with high t_{reg} , smaller C is preferred. $C = 0.3$ and $W_{max} = 0.8 \text{ kg kg}^{-1}$ is preferred for the single stage and two-stage systems for deep dehumidification.

- (3) The reasons for the different requirements of C for low and high relative humidity dehumidification are explained theoretically. As compared with lower C , the pros of higher C is the reduction of t_{reg} because of lower t_d at the same W/W_{max} and ω_d . However, the cons of higher C is that W/W_{max} range should be lower to meet the dehumidification requirement, which may lead to the increase of t_{reg} . The advantages of higher C dominate for high relative humidity dehumidification and higher C is preferred. The disadvantages of higher C dominate for low relative humidity dehumidification and lower C is preferred.
- (4) When W_{max} equals to 0.8 kg kg^{-1} and wheel thickness is 0.2 m , the recommended RS range that works for the regular and deep dehumidification of the single stage and two-stage system under a wide range of working conditions (BSC and WSC) is $10\text{--}15 \text{ r h}^{-1}$. Further analyses showed that the ORS or optimal RS range is mainly influenced by the thickness of the desiccant wheel and the maximum water capacity of the desiccant material. $RS \cdot L \cdot W_{max}$ can be regarded as a constant. ORS or optimal RS range for wheels with different L and material with different W_{max} can be calculated accordingly.

Acknowledgments

The authors appreciate the support from the National Natural Science Foundation of China (No. 51706015) and from the Fundamental Research Funds for the Central Universities (FRF-GF-17-B35).

Appendix A

Heat and mass transfer processes in one of the sinusoidal shape air channels of desiccant wheels are described in the mathematic model. The model is set up based on the following assumptions (Zhang, 2008; Tu et al., 2013b, 2014): (1) the air flow is one-dimensional, and the axial heat conduction and mass diffusion in the fluid are neglected; (2) the air channels are equally and uniformly distributed throughout the wheel; (3) the thermodynamic properties in the solid are constant and uniform; (4) the desiccant and substrate are of the same temperature in the wall thickness direction; and (5) air leakage between the two streams is negligible.

Energy conservation and mass conservation equations of air are as follows:

$$\frac{1}{u_a} \frac{\partial t_a}{\partial \tau} + \frac{\partial t_a}{\partial z} = \frac{4h}{\rho_a c_{pa} u_a d_h} (t_d - t_a) \quad (\text{A1})$$

$$\frac{1}{u_a} \frac{\partial \omega_a}{\partial \tau} + \frac{\partial \omega_a}{\partial z} = \frac{4h_m}{\rho_a u_a d_h} (\omega_d - \omega_a) \quad (\text{A2})$$

h and h_m are expressed in Eqs (A3) and (A4) (Zhang, 2008):

$$h = Nu \frac{k_a}{d_h} \quad (\text{A3})$$

$$h_m = \frac{h}{\rho_a c_{pa} L e^{2/3}} \quad (\text{A4})$$

where Nu is Nusselt number, which, for desiccant wheel, is related to the width and height of the honeycombed channel (Zhang, 2008).

As indicated in Eqs. (A1) and (A2), the air states vary with the wheel angle direction (expressed by τ) and the wheel thickness direction (z direction). Energy and mass conservation equations of the desiccant material are expressed in Eqs. (A5) and (A6):

$$\rho_d \left(c_{pd} + \frac{\rho_{ad} x}{\rho_d} c_{pw} W \right) \frac{\partial t_d}{\partial \tau} + x \rho_{ad} c_{pw} t_d \frac{\partial W}{\partial \tau}$$

$$= k_d \frac{\partial^2 t_d}{\partial z^2} + r_s \rho_{ad} x \frac{\partial W}{\partial \tau} + \frac{4h}{d_h f} (t_a - t_d) \quad (\text{A5})$$

$$\sigma \rho_a \frac{\partial \omega_d}{\partial \tau} + \rho_{ad} \frac{\partial W}{\partial \tau} = \rho_a \sigma D_A \frac{\partial^2 \omega_d}{\partial z^2} + \rho_{ad} D_S \frac{\partial^2 W}{\partial z^2} + \frac{4h_m}{x d_h f} (\omega_a - \omega_d) \quad (\text{A6})$$

where ρ_d and c_{pd} are the equivalent density and the equivalent specific heat capacity of the solid, respectively, which are weighted values of substrate (subscript m) and desiccant material (subscript ad) calculated by Eqs. (A7) and (A8); and f is the frontal area ratio of the solid and air in the control unit, calculated by Eq. (A9):

$$\rho_d = x \rho_{ad} + (1 - x) \rho_m \quad (\text{A7})$$

$$c_{pd} = x^* c_{pad} + (1 - x^*) c_{pm} \quad (\text{A8})$$

$$f = \frac{A_d}{A_a} \quad (\text{A9})$$

Ordinary diffusion D_A and surface diffusion D_S are written as follows (Majumdar, 1998):

$$D_A = \frac{\sigma}{\xi} \left(\frac{1}{D_{AO}} + \frac{1}{D_{AK}} \right)^{-1} : D_{AO} = 1.758 \times 10^{-4} \frac{(t_d + 273.15)^{1.685}}{P_a}, \\ D_{AK} = 97a \left(\frac{t_d + 273.15}{Mol} \right)^{1/2} \quad (\text{A10})$$

$$D_S = \frac{1}{\xi} D_0 \exp \left[-0.974 \times 10^{-3} r_s / (t_d + 273.15) \right] \quad (\text{A11})$$

References

- Al-Alili, A., Hwang, Y.H., Radermacher, R., 2015. Performance of a desiccant wheel cycle utilizing new zeolite material: experimental investigation. *Energy* 81, 137–145.
- Cao, T., Lee, H., Hwang, Y.H., Radermacher, R., Chun, H., 2014. Experimental investigations on thin polymer desiccant wheel performance. *Int. J. Refrigeration* 44, 1–11.
- Chen, C.H., Hsu, C.Y., Chen, C.C., Chiang, Y.C., Chen, S.L., 2016a. Silica gel/polymer composite desiccant wheel combined with heat pump for air-conditioning systems. *Energy* 94 (1), 87–99.
- Chen, C.H., Huang, P.C., Yang, T.H., Chiang, Y.C., Chen, S.L., 2016b. Polymer/alumina composite desiccant combined with periodic total heat exchangers for air-conditioning systems. *Int. J. Refrigeration* 67, 10–21.
- Chung, J.D., Lee, D.Y., Yoon, S.M., 2009. Optimization of desiccant wheel speed and area ratio of regeneration to dehumidification as a function of regeneration temperature. *Sol. Energy* 83, 625–635.
- Dupont, M., Celestine, B., Merigoux, J., Brandan, B., 1994. Desiccant solar air conditioning in tropical climate: I - dynamic experimental and numerical studies of silica gel and activated alumina. *Sol. Energy* 52 (6), 509–517.
- Ge, T.S., Li, Y., Dai, Y.J., Wang, R.Z., 2010. Performance investigation on a novel two-stage solar driven rotary desiccant cooling system using composite desiccant materials. *Solar Energy* 84 (2), 157–159.
- Jain, S., Dhar, P.L., 1995. Evaluation of solid-desiccant-based evaporative cooling cycles for typical hot and humid climates. *Int. J. Refrigeration* 18 (5), 287–296.
- Jeong, J., Yamaguchi, S., Saito, K., Kawai, S., 2010. Performance analysis of four-partition desiccant wheel and hybrid dehumidification air-conditioning system. *Int. J. Refrig.* 33 (3), 496–509.
- Jia, C., Dai, Y., Wu, J., 2006a. Experimental comparison of two honeycombed desiccant wheels fabricated with silica gel and composite desiccant material. *Energy Convers. Manag.* 47, 2523–2534.
- Kodama, A., Hirayama, T., Goto, M., Hirose, T., Critoph, R.E., 2001. The use of psychometric charts for the optimisation of a thermal swing desiccant wheel. *Appl. Therm. Eng.* 21 (16), 1657–1674.
- Jia, C.X., Dai, Y.J., Wu, J.Y., Wang, R.Z., 2006b. Experimental comparison of two honeycombed desiccant wheels fabricated with silica gel and composite desiccant material. *Energy Convers. Manag.* 47 (15–16), 2523–2534.
- Lee, J., Lee, D.Y., 2012. Sorption characteristics of a novel polymeric desiccant. *Int. J. Refrigeration* 35, 1940–1949.
- Majumdar, P., 1998. Heat and mass transfer in composite desiccant pore structures for dehumidification. *Sol. Energy* 62 (1), 1–10.
- Majumdar, P., Worek, W.M., 1989. Combined heat and mass transfer in a porous adsorbent. *Energy* 14 (3), 161–175.
- Pesaran, A.A., 1980. Air dehumidification in packed silica gel bed M.S. Thesis. University of California, Los Angeles.

- Pesaran, A., 1983. Moisture Transport in Silica Gel Particle Beds. University of California, Los Angeles.
- Ramzy, A.K., Kadoli, R., 2011. Improved utilization of desiccant material in packed bed dehumidifier using composite particles. *Renew Energy* 36 (2), 732–742.
- Ruivo, C.R., Angrisani, G., Minichiello, F., 2015. Influence of the rotation speed on the effectiveness parameters of a desiccant wheel: an assessment using experimental data and manufacturer software. *Renew. Energy* 76, 484–493.
- Ruivo, C.R., Goldsworthy, M., Intini, M., 2014. Interpolation methods to predict the influence of inlet airflow states on desiccant wheel performance at low regeneration temperature. *Energy* 68, 765–772.
- Tu, R., Hwang, Y.H., Ma, F., 2017. Performance analysis of a new heat pump driven multi-stage fresh air handler using solid desiccant plates. *Appl. Therm. Eng.* 117 (5), 553–567.
- Tu, R., Liu, X.H., Hwang, Y.H., Ma, F., 2016. Performance analysis of ventilation systems with desiccant wheel cooling based on exergy destruction. *Energy Convers. Manag.* 123, 265–279.
- Tu, R., Liu, X.H., Jiang, Y., 2013a. Heat and mass transfer analysis and performance comparison for different solid dehumidification methods. *CIESC J.* 64 (6), 1939–1947.
- Tu, R., Liu, X.H., Jiang, Y., 2013b. Performance comparison between enthalpy recovery wheels and dehumidification wheels. *Int. J. Refrigeration* 36 (8), 2308–2322.
- Tu, R., Liu, X.H., Jiang, Y., 2014. Performance analysis of a two-stage desiccant cooling system. *Appl. Energy* 13, 1562–1574.
- Tu, R., Liu, X.H., Jiang, Y., 2015a. Lowering the regeneration temperature of a rotary wheel dehumidification system using exergy analysis. *Energy Convers. Manag.* 89 (1), 162–174.
- Tu, R., Liu, X.H., Jiang, Y., 2015b. Irreversible processes and performance improvement of desiccant wheel dehumidification and cooling systems using exergy. *Appl. Energy* 145, 331–344.
- Tu, R., Liu, X.H., Jiang, Y., Ma, F., 2015c. Influence of the number of stages on the heat source temperature of desiccant wheel dehumidification systems using exergy analysis. *Energy* 135 (5), 379–391.
- Tu, R., Qu, S.L., Ma, F., 2015d. Characteristics of outdoor air dehumidifier combined with heat pump system and solid desiccant plates. *CIESC J.* 66 (12), 4796–4805.
- Vandenbulk, E., Mitchell, J.W., Klein, S.A., 1985. Design theory for rotary heat and mass exchangers-II. Effectiveness-number-of-transfer-units method for rotary heat and mass exchangers. *Int. J. Heat Mass Tran.* 28 (8), 1587–1595.
- White, S.D., Goldsworthy, M., Reece, R., Spillmann, T., Gorur, A.D., Lee, Y., 2011. Characterization of desiccant wheels with alternative materials at low regeneration temperatures. *Int. J. Refrigeration* 34, 1786–1791.
- Yadav, L., Yadav, A., 2016. Mathematical investigation of purge sector angle for clockwise and anticlockwise rotation of desiccant wheel. *Appl. Therm. Eng.* 93, 839–848.
- Zhang, H., Niu, J.L., 1999. Two-stage desiccant cooling system using low-temperature heat. *Build. Serv. Eng. Res. Technol.* 20 (2), 51–55.
- Zhang, L.Z., 2008. Total Heat Recovery: Heat and Moisture Recovery from Ventilation Air. Nova Science Publisher, New York.